Consequences of lack of β1 integrin gene expression in mice

Reinhard Fässler[1,2] and Michael Meyer[3]

[1]Max-Planck-Institut für Biochemie and [3]Max-Planck-Institut für Psychiatrie, 82152 Martinsried, Germany

β1 integrins are cell-surface receptors that mediate cell–cell and cell–matrix interactions. We have generated a null mutation in the gene for the β1 integrin subunit in mice and embryonic stem (ES) cells. Heterozygous mice are indistinguishable from normal littermates. Homozygous null embryos develop normally to the blastocyst stage, implant, and invade the uterine basement membrane but die shortly thereafter. Using β1 integrin-deficient ES cells we have established chimeric embryos and adult mice. Analysis of the chimeric embryos demonstrated the presence of β1 integrin-deficient cells in all germ layers indicating that β1–null cells can differentiate and migrate in a context of normal tissue. When evaluated at embryonic day 9.5 (E9.5), embryos with a β1–null cell contribution below 25% were developing normally, whereas embryos with a contribution above this threshold were distorted and showed abnormal morphogenesis. In adult chimeric mice β1 integrin-deficient cells failed to colonize liver and spleen but were found in all other tissues analyzed at levels from 2%–25%. Immunostaining of chimeric mice showed that in cardiac muscle, there were small, scattered patches of myocytes that were β1–null. In contrast, many myotubes showed some β1–null contribution as a result of fusion between wild-type and mutant myoblasts to form mixed myotubes. The adult chimeric brain contained β1–null cells in all regions analyzed. Also, tissues derived from the neural crest contained β1 integrin-deficient cells indicating that migration of neuronal cells as well as neural crest cells can occur in the absence of β1 integrins.

[*Key Words*: β1 integrin; gene targeting; implantation; cell migration]

Received April 3, 1995; revised version accepted June 15, 1995.

Integrins are a large family of cell-surface receptors (Hynes 1992). They are composed of α and β subunits that are noncovalently associated and integrated into the plasma membrane. The extracellular domain of both subunits interacts with cells as well as components of the extracellular matrix such as laminin, fibronectin, and collagens. These interactions have a direct influence on important cellular events, including shape, migration, and differentiation of cells. Many if not all of these effects are believed to be triggered by the ability of the cytoplasmic domain of integrins to associate with and reorganize the actin cytoskeleton (Sastry and Horwitz 1993). Such associations may also be involved in signal transduction processes. The β1 integrin subunit can associate with at least 10 different α subunits and thus forms the largest subfamily of integrins. Although members of this family are expressed on all cells their composition is cell type specific. It is widely believed that this cell type-specific composition of β1 integrins is particularly important in the embryo where they confer adhesive identities to cells and provide necessary positional information for morphogenesis (DeSimone 1994).

[2]Corresponding author.

During all stages of the preimplantation period of the mouse, β1 integrin mRNA or protein can be detected (Damsky et al. 1993). The α6β1 integrin on oocytes recently has been shown to serve as receptor for sperm binding (Almeida et al. 1995). Further functional analysis of integrins with blastocysts in vitro has suggested that they may promote trophoblast outgrowth during implantation (Richa et al. 1985; Armant et al. 1986; Sutherland et al. 1988). In amphibian embryos, the inhibition of integrin function by the injection of arginine–glycine–aspartic acid (RGD) peptides completely blocks mesodermal migration and entry into the blastocoel (Thiery et al. 1985; Darribere et al. 1988). Similarly, mice carrying a null mutation in the α5 integrin gene show reductions in mesodermal structures, particularly in the posterior trunk region of the developing embryo (Yang et al. 1993). Studies employing organ cultures, as well as injections of antibodies and RGD peptides implicate β1 integrins in neural crest migration in amphibians and birds (Thiery et al. 1985; Bonner-Fraser 1986). Members of the β1 integrin family have also been suggested to promote neuroblast migration (Galileo et al. 1992) as well as neurite outgrowth (Letourneau et al. 1988; Tomaselli et al. 1988), somitogenesis (Drake et al. 1992a), formation of myotubes (Menko and Boettiger 1987;

Rosen et al. 1992), and vasculogenesis (Drake et al. 1992b). In a recent study it has been reported that in mice lacking α4 integrin the allantois fails to fuse with the chorion (Yang et al. 1995). In addition, these mice show an abnormal development of the epicardium and coronary vessels leading to cardiac hemorrhage. Interestingly, similar placental and cardiac defects have been observed in embryos lacking vascular cell adhesion molecule (VCAM-1)(Gurtner et al. 1995; Kwee et al. 1995), which is the counter-receptor of α4β1 integrin.

In this paper we report studies on the in vivo functions of the β1 integrin subunit. We have used homologous recombination in embryonic stem (ES) cells to inactivate the β1 integrin gene and generated strains of mice deficient in β1 integrin. Furthermore, we have used β1 integrin-deficient ES cells (Fässler et al. 1995) to generate chimeric mice composed of wild-type and β1 integrin-deficient descendent cells. Analyses of these mouse strains support some of the proposed functions of β1 integrins but not others.

Results

Generation of β1 integrin-deficient mice

Figure 1A shows both targeting vectors used to disrupt the β1 integrin gene in ES cells. The first vector consists of 12 kb of genomic DNA that contains a promotorless neomycin gene cloned in-frame to the ATG of β1 integrin. The second targeting vector contains a promotorless β-galactosidase–neomycin fusion (*geo*) gene flanked by 4 and 6 kb of genomic DNA.

Both targeting vectors were transfected separately into the D3 ES cell line (Doetschman et al. 1985) by electroporation. In addition, the targeting vector containing the promotorless *geo* gene was introduced into the R1 ES cell

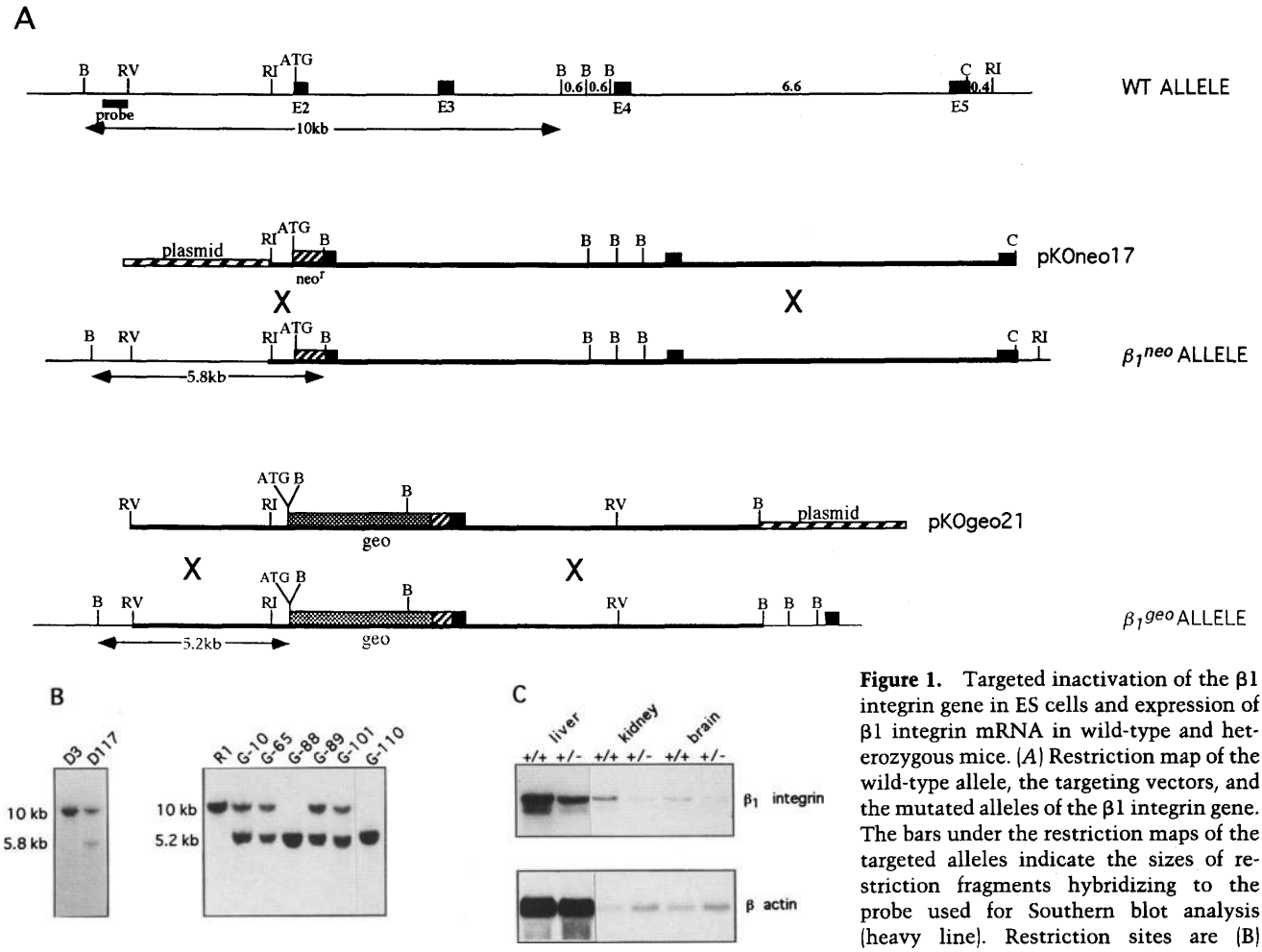

Figure 1. Targeted inactivation of the β1 integrin gene in ES cells and expression of β1 integrin mRNA in wild-type and heterozygous mice. (*A*) Restriction map of the wild-type allele, the targeting vectors, and the mutated alleles of the β1 integrin gene. The bars under the restriction maps of the targeted alleles indicate the sizes of restriction fragments hybridizing to the probe used for Southern blot analysis (heavy line). Restriction sites are (B) *Bam*HI; (RI) *Eco*RI; (RV) *Eco*RV; (C) *Cla*I. (*B*) Southern blot analysis of targeted cells. The 10-kb fragment was derived from the wild-type allele. A novel 5.8 kb for the $\beta 1^{neo}$ allele and 5.2 kb for the $\beta 1^{geo}$ allele was derived from the targeted locus, respectively. (*C*) Total RNA was isolated from liver, kidney, and brain of 3-week-old wild-type and heterozygous mice, separated and probed with oligolabeled mouse cDNAs specific for β1 integrin and β-actin.

line (Nagy et al. 1993). Cell clones containing a disrupted β1 integrin allele were identified by Southern blot analysis using a probe derived from sequences outside the targeting vector (Fig. 1A,B). Among 59 clones electroporated with the *neo* construct, 5 showed homologous recombination resulting in a targeting frequency of 8% *neo*-resistant D3 clones. As reported earlier, D3 ES cells electroporated with the *geo*-containing targeting vector resulted in 104 G418-resistant ES cell clones, of which 58 were heterozygous and 1 homozygous for the β1 integrin mutation (Fässler et al. 1995).

Electroporation of R1 cells with the *geo*-containing targeting vector resulted in 119 G418-resistant clones. Southern blot analysis identified 54 clones with a single knockout and 2 clones with a double knockout, respectively. Whereas both double knockout clones had normal chromosomal contents, one clone showed an additional integration of the targeting vector when hybridized with the *neo* probe (data not shown). The targeting frequency with the *geo*-containing vector was one in approximately two G418-resistant clones in both experiments. Interestingly, selection of $\beta1^{+/-}$ ES cell clones in high concentrations (2 mg/ml) of G418 did not yield β1-negative ES cells (data not shown).

β1 integrin-deficiency causes lethality shortly after embryo implantation

Cell line D117 (D3 cell clone disrupted by *neo*) and cell lines G10, G11, G20, G65 (R1 cell clones disrupted by *geo*) were used to generate chimeric males that transmitted the mutant allele to their progeny. Mice heterozygous for the mutation in the β1 integrin gene were identified by Southern blot analysis of tail DNA. Heterozygous mice appeared normal and were indistinguishable from their wild-type littermates. Northern blot analysis of total RNA derived from liver, kidney, and brain revealed that the β1 integrin mRNA in heterozygous mice is reduced by 50% when compared with wild-type littermates (Fig. 1C).

To obtain mice homozygous for the β1 integrin mutation, heterozygous mice were intercrossed and tail biopsies assayed by Southern blot analysis. Among 438 viable offspring, 294 were identified as heterozygotes (67%) and 144 as wild type (33%). Homozygous β1 integrin mutants were not among the progeny, indicating their early death during development.

To determine the time of embryonic lethality, heterozygous mice were intercrossed and decidua swellings collected at embryonic day 5.5 (E5.5), E6.0, E7.5, E8.5, and E9.5, sectioned, and assayed for *lacZ* activity and β1 integrin expression. Whereas normal (Fig. 2a) or heterozygous (distingiushed by *lacZ* staining) embryos had formed egg cylinders with a proamniotoic cavity at E5.5 and E6.0, β1–null embryos are completely resorbed and only some β1 integrin-deficient trophoblast cells are still visible. Figure 2b shows an E6 β1–null embryo stained for *lacZ* activity and an adjacent section examined for β1 integrin expression (Fig. 2c). Whereas β1 integrin-deficient trophoblast cells can be identified, no cells of the embryo proper are present. Interestingly, no other presumptive β1–null embryo tested at this stage contained such a large number of β1 integrin-deficient trophoblast cells. At later ages (E7.5–E9.5) in sections of 10 of 44 (23%) normal-looking implantation chambers, neither embryos nor cells could be found. Southern blot analysis of DNA derived from E8.5, E9.5, and E10.5 yolk sac, together with embryo tissue (Table 1), further confirmed

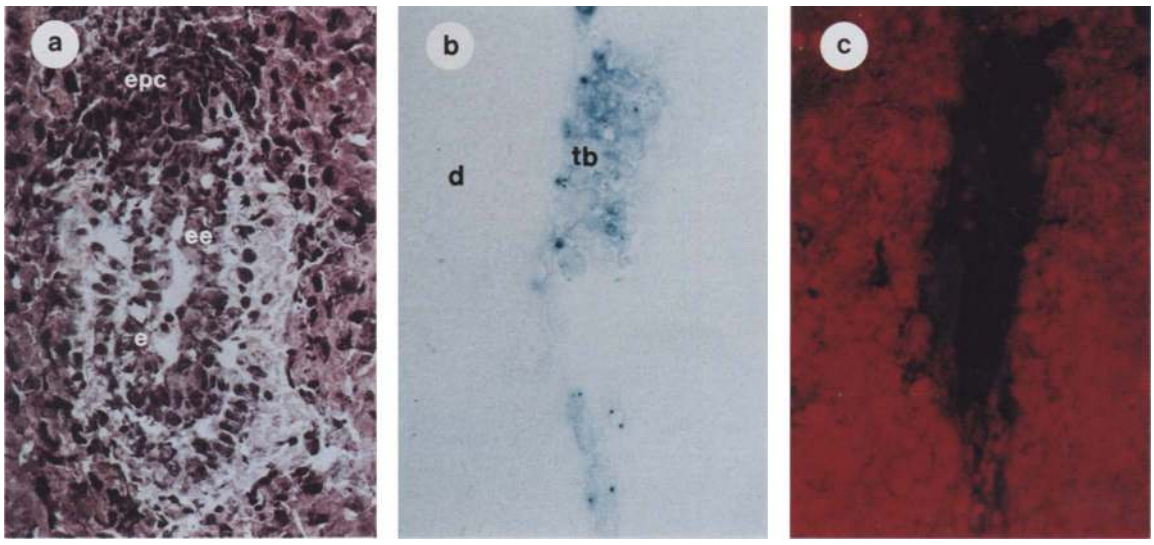

Figure 2. E6 embryos of a heterozygous cross stained for *lacZ* activity and β1 integrin expression. (*A*) Wild-type embryo negative for *lacZ* activity was stained with eosin and hematoxylin; (*b,c*) Section of a β1 integrin-deficient embryo stained for *lacZ* activity (*b*) and an adjacent section immunostained for β1 integrin (*c*). Whereas a bright fluorescence signal was detected in decidual cells, trophoblast cells present at the invasive site stained negative for β1 integrin. No cells of the embryo proper could be detected. (epc) Ectoplacental cone; (ee) extraembryonic ectoderm; (e) ectoderm; (tb) trophoblast cells; (d) decidua.

Table 1. *Progeny of $\beta1^{+/-} \times \beta1^{+/-}$ crosses*

Stage	Assay	+/+	−/+	−/−	Empty decidua
E3.5 blastocysts	IF and *lacZ*[a]	9	21	6	—
E8.5 turned, 8–12 somites	Southern	6	16	0	9
E9.5 turned, 20–25 somites	Southern	12	22	0	10
E10.5 appendages formed	Southern	10	26	0	13
D42 adults	Southern	144	294	0	—

[a]Genotype was determined by immunostaining (IF) and *lacZ* assay.

that normal embryos were either wild type or heterozygous for the β1 integrin null mutation.

To determine whether β1 integrins are essential for the preimplantation period, E3.5 blastocysts were isolated from the uterus of heterozygous females mated with heterozygous males. A total of 36 blastocysts were isolated and found to be phenotypically indistinguishable from one another. After removal of the zona pellucida these blastocysts were first immunostained for β1 integrin and analyzed afterwards for *lacZ* activity. Among 36 blastocysts, there were 6 blastocysts negative for β1 integrins (16%, homozygous mutant) (Fig. 3). The β1 integrin-expressing blastocysts could be grouped further in 9 blastocysts, which showed no *lacZ* activity (25%, wild type) and 21 blastocysts with *lacZ* activity (58%, heterozygous mutant; Fig. 3).

These results indicate that the β1 integrin gene is not essential for embryonic development up to the blastocyst stage (E3.5). Furthermore, embryos lacking β1 integrin attach to the uterine epithelia and invade the stroma but die shortly thereafter.

Generation of chimeric animals using β1 integrin-deficient ES cells

Two independent β1–null ES cells, one derived from D3 (G201; Fässler et al. 1995) and the other from R1 (G110; see Fig. 1), were injected into wild-type C57BL/6 blastocysts and transferred into foster mice. Embryos were collected from decidua swellings at E6.5 to E10.5 at daily intervals and assayed for *lacZ* activity. Surprisingly, many of the normally developed embryos contained *lacZ*-positive areas. In whole-mount E6.5 embryos, the egg cylinder of all 11 embryos analyzed showed an extensive contribution of β1–null cells (Fig. 4a).

Histological sections of E8.5 embryos revealed that labeled cells could be found in all germ layers (Fig. 4b). At E8.5, E9.5, and E10.5, two types of embryos became apparent: normally developed embryos with *lacZ* activity in ~5%–10% of the cells (Fig. 4b–d), and malformed embryos with a high contribution of *lacZ*-positive cells (Fig. 4e,f). In the particular example shown, the embryo appeared as a homogenous mass of blue cells. A similar distorted embryo at E8.5 was sectioned and stained for *lacZ* activity. Figure 4f shows the embryo as a clump of

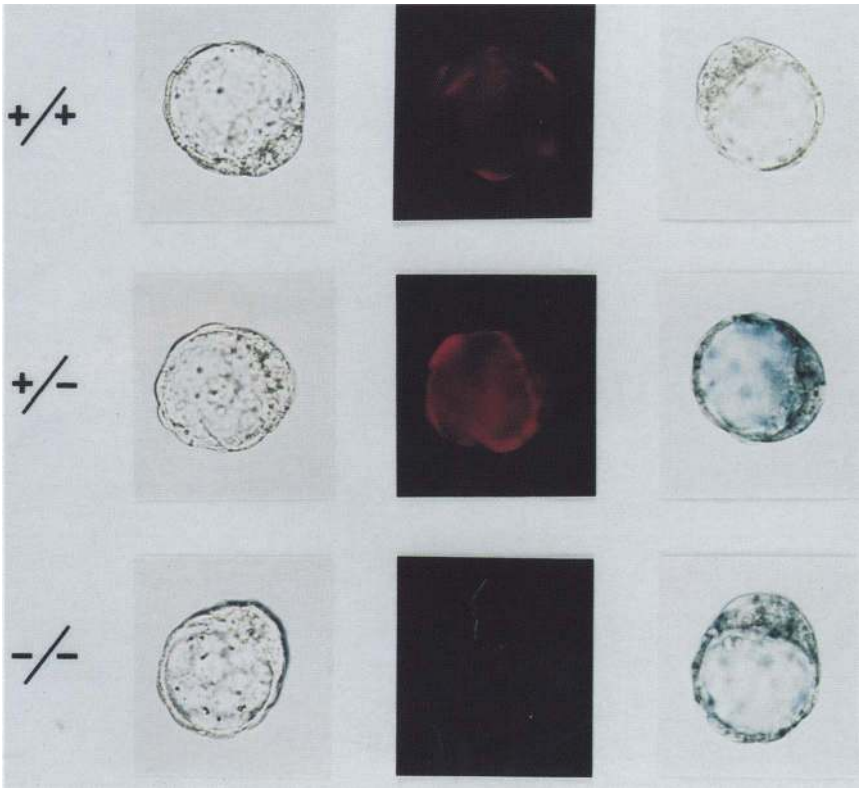

Figure 3. β1 integrin and *lacZ* expression in blastocysts of heterozygous crosses. Blastocysts were treated with acid Tyrode's solution, incubated for 6hr at 37°C, fixed in 4% paraformaldehyde, photographed (lane *1*), immunostained individually for β1 integrin, and photographed in solution (lane *2*). Afterwards blastocysts were assayed individually for *lacZ* activity and photgraphed again (lane *3*). β1–null blastocysts are indistinguishable from wild-type or heterozygous blastocysts.

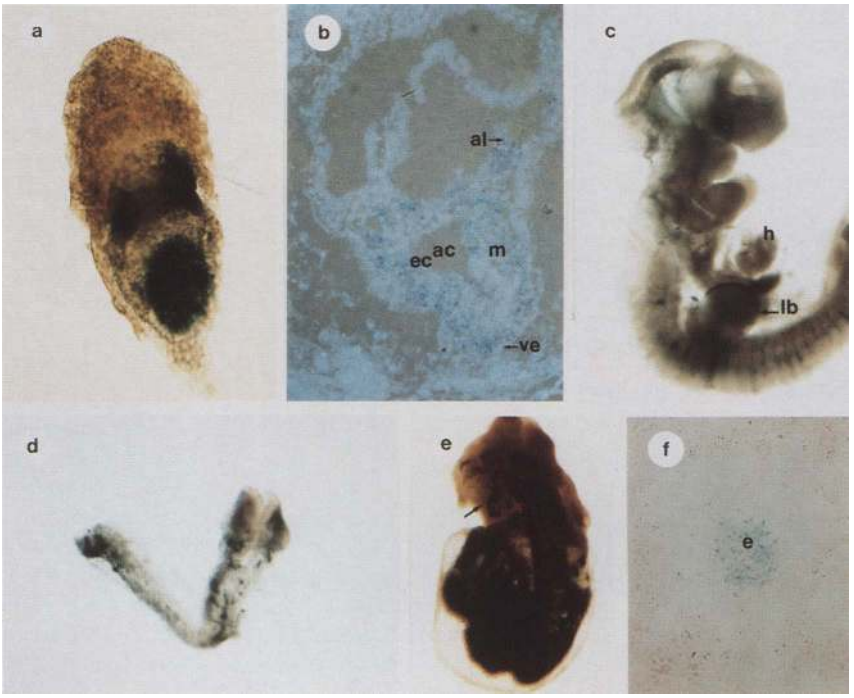

Figure 4. Chimeric embryos analyzed at various developmental stages for the presence of β1–null cells. (*a*) An E6.5 embryo stained for *lacZ* activity shows the presence of β1–null cells in the epiblast. (*b*) Sagittal section of an E8.5 embryo. *lacZ*-Positive cells are present in all germ layers and allantois (al). (*c*) E10.5 embryo with *lacZ* staining in the heart, between the vertebra anlage, in the limb bud, and brain tissue. (*d–f*) E8.5 embryos from the same litter. The embryo in *d* shows normal morphogenesis with low contribution of *lacZ*-positive cells. The embryo in *e* is inside the yolk sac, shows a high β1–null cell contribution, and is malformed. Parasagittal section of a malformed embryo (*f*) demonstrates the absence of gastrulation and neurulation. Embryo *e* consists of a mixture of *lacZ*-positive and -negative cells. Arrow in *e* shows blue staining in the ectoplacental cone. (ec) Ectoderm; (m) mesoderm; (ve) visceral endoderm; (lb) limb bud; (h) heart.

lacZ-positive and -negative cells without signs of gastrulation or neurulation having occurred. This indicates that morphogenesis cannot occur at high contribution of β1 integrin-deficient cells. In ~20% of the embryos *lacZ*-positive cells were also found in the ectoplacental cone (see arrow in Fig. 4e and data not shown). Furthermore, *lacZ* staining of injected β1–null cells revealed that the extent of chimerism varied both from one embryo to another and one region to another within a single embryo. The only region in the E10.5 embryos that did not appear to be colonized by *lacZ*-positive cells was the apical ectodermal ridge. In many of the limb buds analyzed, however, strong *lacZ* labeling was seen just beneath this region (Fig. 4c)

To determine more precisely the percent contribution of mutant cells in normally and abnormally developed E9.5 chimeric embryos the ratio of ES cell-specific versus host blastocyst-specific glucose-6-phosphate isomerase (GPI) isoenzymes was determined in 12 embryos generated with the G201 cell line ($\beta1^{-/-}$; D3-derived). The two chimeric embryos that appeared normal contained 8% and 24% β1–null cells, respectively, whereas the four chimeric embryos that were malformed had ES cell contributions of 28%, 32%, 56%, and 73% (Table 2). Similar results were obtained when G110 cells ($\beta1^{-/-}$; R1 derived) were used to generate chimeric embryos (Table 2). In control experiments heterozygous mutant cells (G20; R1 derived) were injected. Ten embryos were analyzed, of which all appeared normal and showed up to 74% ES cell contribution (Table 2).

Taken together, these data demonstrate clearly that $\beta1^{-/-}$ cells can participate in normal embryonic development. A high contribution of $\beta1^{-/-}$ cells, however, is associated with distorted development and lethality.

Table 2. *Evaluation at E9.5 of the frequency of normal development and chimerism among blastocysts injected with homozygous and heterozygous β_1-deficient ES cells*

ES cell line	Number of blastocysts injected	Number of embryos			Percent 129-derived GPI in chimeras (*n*)	
		resorbed	retarded	normal	retarded	normal
G-201 (−/−)	12	0	7	5	46.0 (4)[a]	8, 24 (20)
G-110 (−/−)	16	1	6	9	43.5 (6)[b]	8.8 (4)[c]
G-20 (+/−)	18	3	0	15	0	59.8 (10)[d]

[a]Individual values were 28%, 32%, 56%, and 73%.
[b]Individual values were 7%, 13%, 42%, 59%, 68%, and 72%.
[c]Individual values were 4%, 5%, 8%, and 18%.
[d]Individual values were 17%, 23%, 39%, 42%, 48%, 51%, 58%, 63%, 67%, and 74%.

Tissue contribution of β1$^{-/-}$ cells in mature animal tissues

Most surprisingly, chimeric β1$^{-/-}$ animals were readily obtained (Fig. 5a). The contribution of mutant cells in chimeric animals as estimated from the agouti coat color ranged from ~2%–25%. In contrast, heterozygous cells contributed up to 95% to the coat color of chimeric animals.

The mean contribution of ES cells to various tissues in chimeric β1$^{-/-}$ and β1$^{+/-}$ mice was analyzed further by determining the GPI pattern (Table 3). Clearly, β1$^{-/-}$ cells were found in most tissues. Brain hemispheres and skeletal muscle showed the highest β1–null cell contribution and matched or even exceeded the estimated agouti coat color in the β1$^{-/-}$ chimeric animals. Much lower levels of 129 cell-derived GPI isoenzymes were found in lung, kidney, gut, heart, adrenal gland, and cerebellum. However, 129 cell-derived GPI was never detected in liver and spleen.

Although the GPI analysis indicated the presence of β1 integrin-deficient cells in many tissues of adult chimeras, these results could not show which cell types in a given tissue were β1 integrin-deficient and whether differentiation of the null cells occurred normally. Therefore, *lacZ* expression was determined in a number of tissues that were shown to be free of endogenous β-galactosidase activity in normal control mice. Endogenous β-galactosidase activity could be blocked completely in some tissues (e.g., brain) by staining at pH of 7.6 and 30°C but not in others (kidney, gut, testis, thyroid gland).

In agreement with the GPI analyses we could not detect *lacZ*-labeled cells in liver. However, in all other tissues investigated thus far, *lacZ*-expressing cells were present and were indistinguishable from wild-type cells. For example, unambigous *lacZ*-positive cells were detected among chondrocytes of rib cartilage (Fig. 5b) that were morphologically indistinguishable from unstained cells in the same area. Skin samples from four chimeric animals were examined and were found to contain many labeled cells in various regions (Fig. 5c). Many mesenchymal cells in the dermis as well as the subcutis expressed *lacZ*. In some specimens, sweat glands and sebaceous glands (especially in tail skin; data not shown) contained *lacZ*-positive cells. A comparison of *lacZ* staining in cardiac and skeletal muscle was particularly interesting (Fig. 6). As suggested by the GPI data, the contribution of β1-negative cells was relatively high in skeletal muscle (Fig. 6a) and low in cardiac muscle (Fig.

Table 3. *Tissue contribution of β1 integrin-deficient cells in chimeric mice as determined by GPI assay*

	Percent contribution of						
	β1$^{-/-}$ mouse no.				β1$^{+/-}$ mouse no.		
Tissue	1	2	3	4	1	2	3
Brain hemisphere	9	7	3	3	52	51	37
Cerebellum	10	<2	<2	<2	48	42	28
Lung	<2	3	<2	<2	33	39	27
Heart	<2	3	<2	<2	49	17	28
Liver	0	0	0	0	17	21	44
Spleen	0	0	0	0	51	43	12
Kidney	<2	4	<2	5	83	46	17
Adrenal glands	4	3	<2	<2	87	68	49
Gut	7	3	13	9	12	27	7
Testis	<2	<2	0	6	11	21	18
Skeletal muscle	29	12	8	14	>95	64	54
Coat color[a]	20	15	5	5	>95	70	40

[a]Coat color was judged by eye.

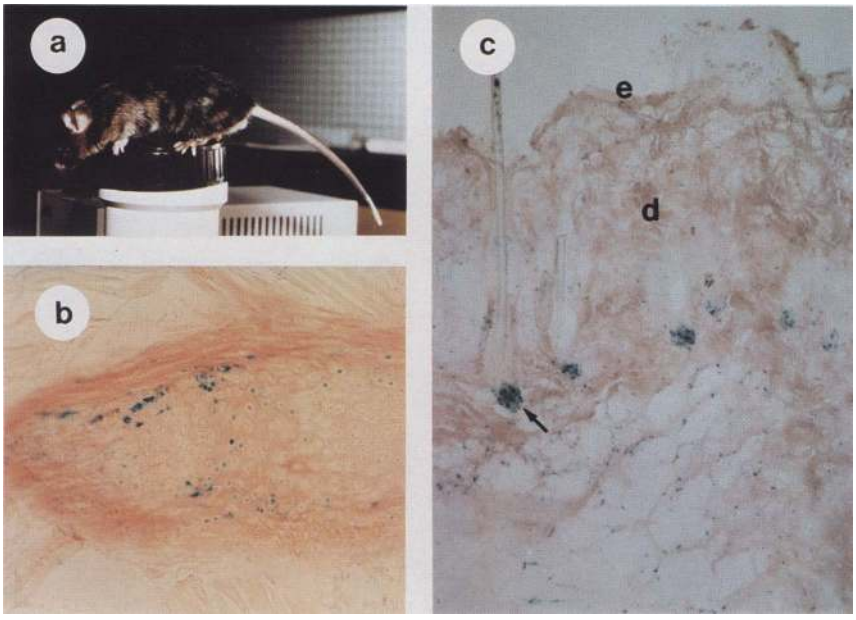

Figure 5. (*a*) Four-month-old β1–null chimeric mouse. (*b*) Section of rib cartilage showing chondrocytes with *lacZ* activity. (*c*) Section of skin derived from an agouti area of a β1–null chimeric mouse. Sweat glands (arrow) exhibit extensive *lacZ* activity. Many of the mesenchymal cells in the dermis are *lacZ*-positive. (e) Epidermis; (d) Dermis.

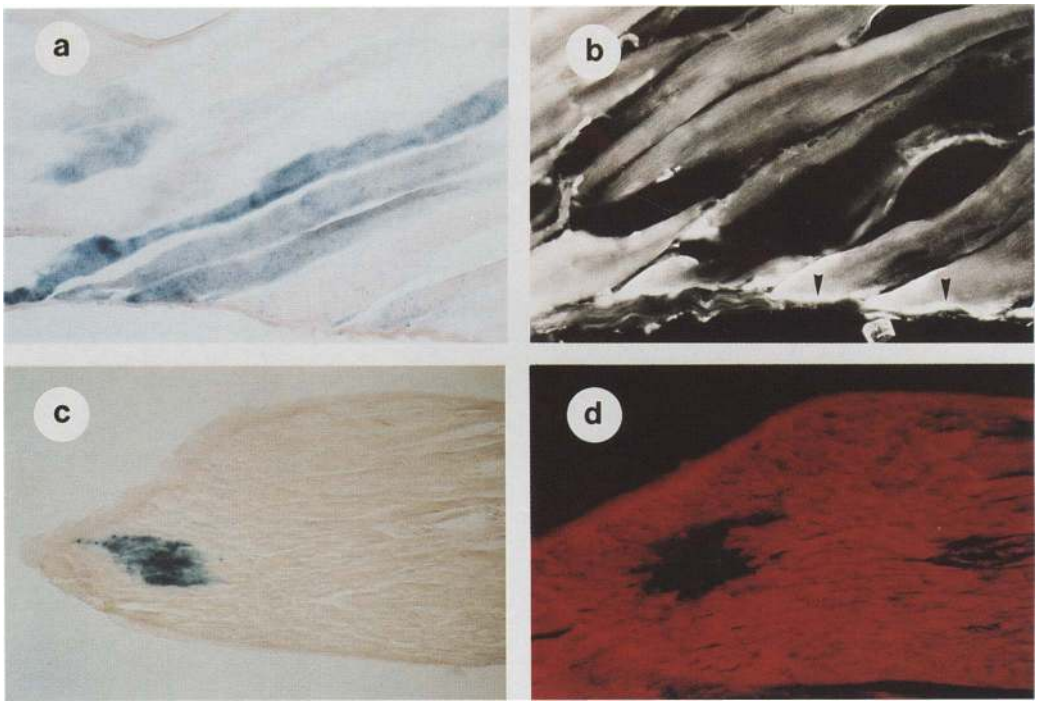

Figure 6. Analysis of skeletal and cardiac muscle from β1–null chimeric mice. Tissue specimen from the triceps muscle (*a*, *b*) was stained for *lacZ* activity and counterstained with eosin. Whereas most of the myotubes contain the *lacZ* product, the degree of staining intensity is different between myotubes. Immunostaining of an adjacent section (*b*) demonstrates the presence of β1 integrin, particularly at the myotendinous junction (arrowheads). (*c*, *d*) Cardiac muscle with a representative area of *lacZ*-positive cells. Tissue specimen was counterstained with eosin. (*c*) Immunostaining of adjacent tissue section demonstrates the absence of β1 integrin in the corresponding *lacZ*-positive area (*d*).

6c). In addition, the patterns of staining were very different. In cardiac muscle, β1-negative cells were present as scattered single cells or as small patches of cells that stained uniformly and intensely for *lacZ*. In contrast, quite a high percentage of myotubes were stained along their entire length, but the staining intensity varied from one myotube to another. This variable pattern suggested that β1 − /*lacZ*$^+$ and wild-type/*lacZ*$^-$ myoblasts had fused with one another. To test this possibility, alternating serial sections were stained with *lacZ* and β1 integrin antibody. Comparison of the staining patterns in adjacent sections indicated clearly that many myotubes were both β1 positive and *lacZ* positive (Fig. 6a,b). In contrast, cardiac muscle cells staining strongly for *lacZ* were negative for β1 integrin (Fig. 6c,d). These results demonstrate that in myotubes β1 integrin deficiency is rescued by wild-type myoblasts. This rescue phenomenon might account for the relatively high chimerism present in skeletal muscle, compared with cardiac muscle and other tissues.

Contribution of β1$^{-/-}$ cells in adult brain and neural crest

To test whether neural crest and neuronal cell migration and/or differentiation were affected by the lack of β1 integrins we undertook a detailed histochemical characterization of different regions of the nervous system in chimeric animals.

Surprisingly, *lacZ*-positive cells were observed in most regions of the central nervous system, including olfactory bulb, cortex, striatum, septum, hippocampus, cerebellum, and spinal cord. Staining in the olfactory bulb was present in the mitral cell layer in cells that could not be distingiushed from *lacZ*-negative mitral cells by neutral red and cresyl violet staining (not shown). *lacZ*-Positive cells were also present in the periglomerular and in the granular cell layer. All layers of the cortex except the molecular layer (layer 1) contained cells with *lacZ* activity (Fig. 7e–g). Both by morphological (size) and staining criteria (Nissl staining, neurofilament heavy chain), these cells are neurons. Interestingly, a big proportion of the *lacZ*$^+$ cortical neurons contained the blue stain at two opposing locations at the periphery of the cell soma (Fig. 7e). The identity of blue cells in striatum, septum, and spinal cord could not be determined with the staining protocols used in this study. In the hippocampus, cells stained for *lacZ* activity were present in the dentate gyrus, the hilar regions of the dentate gyrus, and all sections of the pyramidal cell layer (Fig. 7h,i). Occasionally, blue dots were also observed in regions containing dendrites of pyramidal cells. The staining pattern observed with cresyl violet suggested that granule cells and pyramidal neurons contained the reaction product (data not

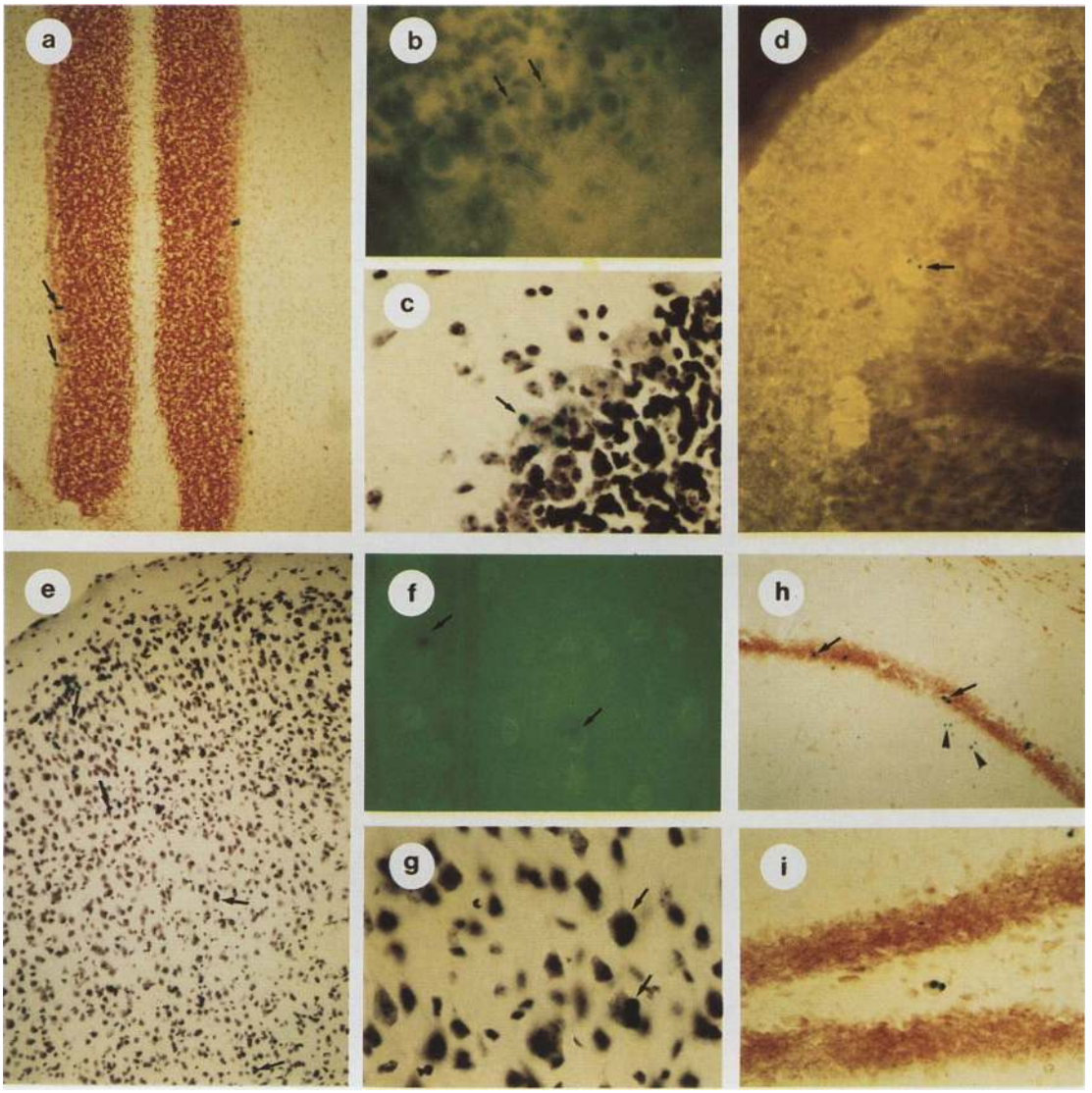

Figure 7. *lacZ* staining in the central nervous system of an adult chimeric mouse. (*a*) *lacZ* staining is present in the Purkinje cell layer (arrows) of the cerebellum. (*b*) Section of the cerebellar cortex stained for MAP5. Arrows point to MAP5 and *lacZ*-positive Purkinje cells. (*c*) High-power view of Purkinje cell layer stained with cresyl violet. A big cell displaying Nissl staining characteristic for Purkinje cells also contains *lacZ* reaction product (arrow). (*d*) Double exposure of a cerebellar section stained with a monoclonal antibody to calbindin D28k and reacted for *lacZ* histochemistry. Dentritic trees and somata of Purkinje cells including the *lacZ*-positive cell (arrow) are calbindin-positive. (*e*) Cortex stained with cresyl violet. Arrows point to *lacZ*-positive cells present in all cortical layers. (*f*) Frontal section through cerebral cortex stained for neurofilamen heavy chain. Arrows indicate neurofilament positive cells also containg the *lacZ* staining. (*g*) High-power view of cortical section stained with cresyl violet. Two cells (arrow) containing *lacZ* staining also display size and Nissl staining characteristics of neurons. (*h*) Sections of the hippocampus show *lacZ*-positive cells in the pyramidal cell layer. In some areas blue dots are found associated with the dentritic fields (arrowheads). In (*i*) the fascia dentata shows *lacZ*-positive hilar neurons. Sections shown in *h* and *i* were counterstained with neutral red.

shown). An interesting cellular expression was observed in the cerebellum, where blue dots were concentrated mainly over Purkinje cells somata (Fig. 7a–c). Occasionally *lacZ*-positive cells were present in the granule cell layer, where, because of the high cell density, the identity of the labeled structures could not be unambigously identified. Blue dots were also present in the deeper part of the molecular layer that contains the dendritic trees of the Purkinje cells. Immunostaining of calbindin D28k, a calcium-binding protein present in differentiated Purkinje cells and microtubule-associated protein 5 (MAP5), could be observed in both *lacZ*-positive and *lacZ*-negative cells (Fig. 7b,d). In addition, Nissl staining did not show any morphological differences between *lacZ*-positive and *lacZ*-negative Purkinje cells (Fig. 7c).

In two of the chimeric animals, analysis was extended

to the neural crest-derived peripheral nervous system. In lumbar dorsal root ganglia blue dots were observed over the somata of medium-sized sensory neurons (Fig. 8a). Additional blue staining was occasionally observed at the periphery of neuronal somata. *lacZ*-positive neurons were also observed in the sympathetic superior cervical ganglion (SCG; data not shown). *lacZ* activity was not detected in sections of the sciatic nerve.

Another neural crest-derived structure is the adrenal medulla. GPI analysis indicated that adrenal glands contain β1 integrin-deficient cells. To determine the location of β1–null cells more specifically, adrenal tissue sections from three chimeric mice were stained for LacZ activity. Both the adrenal cortex and medulla contained blue cells in all three cases. Figure 8, b and c, shows extensive *lacZ* staining in the chromaffin cells present in the adrenal medulla.

Taken together, these results indicate that the lack of β1 integrin does not preclude incorporation of β1–null cells into the neural tube and neural crest-derived tissues in chimeric animals.

Discussion

In this study a genetic approach was used to assess the role of β1 integrins during mouse development. For this purpose, ES cells were modified by homologous recombination to obtain cells and mouse embryos that lack β1 integrin. Mice deficient for β1 integrin exhibit no obvious deficits in their preimplantation development. However, they die shortly after implantation. This result was obtained with five independent ES cell clones, one β1 integrin mutant line containing the *neo* gene, and four mutant lines containing the *geo* gene.

Various members of the β1 integrin family are expressed on the surface of blastomeres throughout the whole preimplantation period (Sutherland et al. 1993). Our results demonstrating normal preimplantation development in the absence of β1 integrins suggest that they are not absolutely required during this period. Almeida et al. (1995) have shown, however, that antibodies against α6β1 integrin block oocyte fertilization in mice, suggesting that this integrin binds to a sperm counter receptor, most likely PH-30, which contains a disintegrin domain (Blobel et al. 1992). The normal fertilization frequency occurring in crosses of heterozygous animals suggests that β1 integrin mRNA must be present in oocytes carrying a null mutation in the β1 integrin gene. This is supported by the presence of mRNA for β1 integrin in normal unfertilized eggs and zygotes as detected by RT–PCR (Sutherland et al. 1993) and by Northern blot analysis (R. Fässler and A. Vasalli, unpubl.). This indicates that β1 integrin mRNA is provided as a maternal message and is thus present on β1–null oocytes.

The results of the present study indicate that the null mutation of the β1 integrin gene results in a recessive lethal periimplantation defect. Furthermore, they show that in the absence of β1 integrins the trophoblast can attach to epithelial cells of the uterus and induce the decidual response. At E5.5 and E6 we found small nests of trophoblast cells in ~25% of the implantation chambers. Antibody staining for β1 integrin revealed that these trophoblast cells lack β1 integrin expression and are the remnants of the β1–null embryos. These findings indicate that β1 integrins are not essential for initial implantation of the embryo. Several other adhesion mechanisms have been postulated. Blastocysts express at least three αv-containing integrins that associate with other β subunits (Damsky et al. 1993; Sutherland et al. 1993). Furthermore, blastocysts express carbohydrates that interact with selectins present on uterine epithelial cells (Brown et al. 1993). Blastocysts express perlecan at the time they become attachment competent (Carson et al. 1993), as well as other proteoglycans that may interact

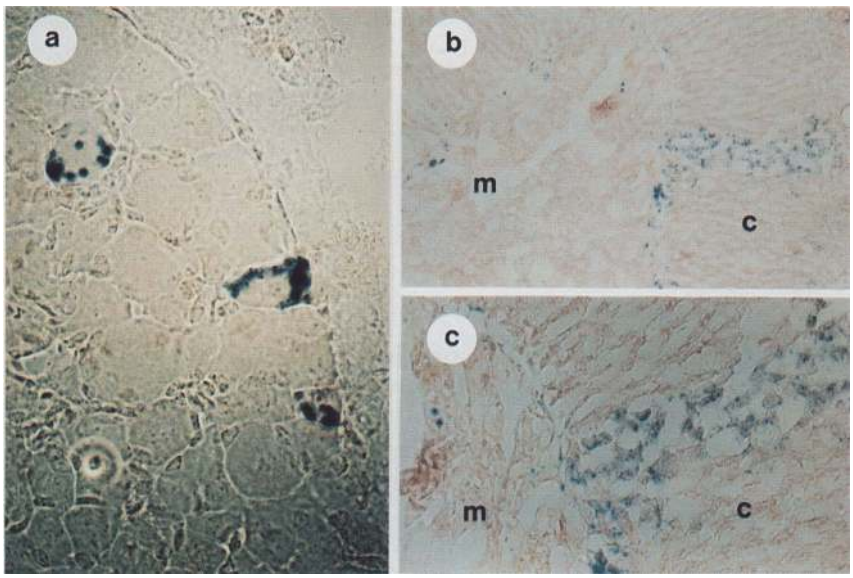

Figure 8. *lacZ*-Positive cells in dorsal root ganglia and medulla of the adrenal gland. (*a*) *lacZ* staining in medium-sized sensory neurons of a lumbar dorsal root ganglion. The small satellite cells surrounding the larger neuronal cell bodies are negative. The section was counterstained weakly with neutral red. (*b*,*c*) Adrenal gland showing β1–null cells in cortex (c) and medulla (m). *c* shows the *lacZ*-positive cells in the medulla at higher magnification.

with uterine epithelial cells and permit interaction with hyaluronic acid, which is present in the extracellular matrix (ECM) of the uterine wall at the site of implantation (Jacobs and Carson 1991; Brown and Papaioannou 1993). Taken together, there are many molecules that could act as adhesive components and thus allow the attachment of β1–null blastocysts to the uterine epithelium.

Interestingly, we could not find cells of the embryo proper in any of the E5.5 and E6 presumptive implantation chambers, indicating that the inner cell mass cells die earlier than trophoblast cells. This finding has been examined further in embryos cultured in vitro (Stephens et al., this issue). In these studies β1–null blastocysts formed normal trophblast outgrowths. Moreover, growth of the inner cell mass was retarded, and ectoderm morphogenesis and migration were defective. A possible explanation for this finding could be that the inner cell mass cells lack necessary signals from the β1–null trophoblast. Alternatively, ICM cells could have retarded growth or die before or soon after differentiation into ectoderm and endoderm because they lack important signals from the surrounding matrix. As discussed in Stephens et al. (this issue), it has been shown that the contact of normal endothelial and epithelial cells with ECM is important for cell growth and survival (Ruoslahti and Reed 1994). Because these reports implicate integrins in programmed cell death we are currently trying to assess whether such mechanisms play a role in the transition of inner cell mass cells to ectodermal and endodermal cells in vivo and are responsible for the death of β1 integrin-deficient embryos.

The early death of β1 integrin embryos restricted the functional analyses to the period before and around implantation. Ideally, one would like to investigate the consequences of β1 integrin deficieny at later stages of development to assess the migratory and differentiation capacity of cells lacking β1 integrins. An attractive way of doing this is to introduce a conditional null mutation into the β1 integrin gene. Alternatively, β1 integrin-deficient ES cells can be injected into normal blastocysts and the resulting chimeric embryos can be analyzed. We have reported earlier that we could generate β1 integrin-deficient ES cells and have shown that these cells are able to integrate themselves into the inner cell mass (Fässler et al. 1995). To be sure that these initial findings were a general property of β1–null cells and not an artifact of the selection procedure, we have now established two more β1 integrin-deficient ES cell clones, both derived from the R1 ES cell line. Both of these mutant clones could contribute to the epiblast at E6.5 and were found in all three germ layers at E8.5.

When we analyzed chimeric embryos at E9.5 two types of embryos could be recognized. First, embryos that contained low percentages of β1 integrin-deficient cells and still appear normal; and second, embryos that had high contributions of *lacZ*-expressing cells and were completely distorted. Analysis of the GPI patterns (Table 2) in these E9.5 embryos demonstrated that the maximum contribution of $\beta1^{-/-}$ cells compatible with normal development in chimeras is below 20%–25%. At this time, we can only speculate why higher contributions of β1 integrin-deficient ES cells are associated with abnormal development. Because integrins can transmit growth signals, a high contribution of mutant cells may lead to growth retardation that is incompatible with normal development. An alternative explanation is that mutant cells are unable to form a proper supramolecular network of matrix proteins resulting in inadequate cell migration and differentiation. Such deficiencies could be compensated for by normal cells when the contribution of mutant cells is below a certain threshold. We have indications for the latter explanation from in vitro experiments with β1 integrin-deficient cell lines that have a severely impaired ability to assemble fibronectin into fibrils (S. Johansson and R. Fässler, in prep.).

In a variety of experiments it has been shown that β1 integrin function is important for cell migration. Antibodies or synthetic peptides that block β1 integrins inhibit migration of neural crest cells and myoblasts in vivo (Thiery et al. 1985; Jaffredo et al. 1988). Retrovirally transduced β1 integrin antisense RNA blocks neuroblasts migration in vivo (Galileo et al. 1992). This block in neuroblast migration could be achieved by reducing β1 integrin mRNA levels by 50%. However, our analysis of chimeric embryos presented here demonstrates clearly that β1 integrin-deficient cells are present in most tissues, including those dependent on extensive migration. These conflicting results most likely indicate that there is a crucial difference between the ablation of integrin function in differentiated cells versus the genetic loss of integrin from the outset of development. In the latter cases, embryos might be able to activate dormant, alternative pathways that can compensate for the deficiency sufficiently to enable migration as well as differentiation. Such an activation may, however, not be possible in groups of cells that have already organized themselves in the presence of the integrins. The same mechanisms might also account for the fact that in some cases mice carrying mutations in genes thought to be important for many morphogenetic events do not show a pathological phenotype.

Interestingly, all chimeras analyzed showed a high β1–null cell contribution in skeletal muscle and no contribution or one below the detection limit in liver and spleen. The latter finding most likely indicates that hepatocyte differentiation is dependent on the presence of β1 integrins. Hematopoetic cells might need β1 integrins to colonize their target organs, although a block in differentiation cannot be excluded at this time. Alternatively, it is also possible that we missed chimeras in which mutant cells have colonized these organs. To exclude such possibilities many more experiments such as recombination activating gene (RAG)-deficient blastocyst complementation (Chen et al. 1994) or conditional knockouts (Gu et al. 1994) have to be performed. All other tissues analyzed contained at least a few β1 integrin-deficient cells, which were often barely detectable by GPI determinations.

To test which cell types are formed and whether they

can differentiate normally without β1 integrins, we stained several tissues for *lacZ* expression. *lacZ* staining identified small numbers of chondrocytes, different cell types in skin, neuronal cells of different brain regions, and cardiac muscle cells as well as relatively high numbers of skeletal muscle fibers as β1 integrin deficient. None of these cell types exhibited any obvious morphological abnormalities. Antibody staining clearly showed that *lacZ*-positive cardiac muscle cells lack β1 integrin subunits, whereas myotubes express them. Apparently, the lack of β1 integrin is compensated after fusion of mutant and normal myoblasts.

The phenotype we have observed for β1 integrin-deficient cells in chimeric mice is unexpected. β1 integrins are found on the surface of almost all cells and have been implicated in many important cellular functions. Therefore it was surprising that β1–null cells were present in so many tissues and that they could differentiate. At present we do not know how these mutant cells migrate into tissues and whether they can fullfill their normal functions after differentiation. Migration might be achieved with integrins other than β1 and/or by using non-integrin cell-surface receptors or cell–cell interactions of mutant cells with normal cells that could allow passive migration. The considerable reduction in the number of *lacZ*-positive cells from ~20%–5% observed during development of chimeras was a significant observation in all experiments. This indicates an increasing failure in passive migration and/or increasing loss of mutant cells due to apoptosis. These data are reminiscent of earlier findings demonstrating that the anti-apoptotic effects of neurotrophins depend on the appropriate extracellular matrix in vivo and in vitro (Kalcheim et al. 1987; Ernsberger et al. 1989). Further support for passive migration comes from the observation that none of the tissues analyzed contained large groups of mutant cells; rather, they contained single cells or small clusters. This suggests that the β1 mutant cells can undergo morphogenesis only in the context of normal cells.

Materials and methods

Construction of targeting vectors

Two targeting vectors were made for the disruption of the β1 integrin locus. The first targeting vector contained a promotorless β-galactosidase–neomycin fusion DNA (*geo*) cassette (pKO*geo*21) in-frame to the start codon of β1 integrin and has been described previously (Fässler et al. 1995).

The second targeting vector containing a promotorless *neo* cassette was constructed from the same isogenic DNA as pKO*geo*21. A 10.5-kb *Eco*RI–*Cla*I fragment containing exon 2, exon 3, exon4, and most of exon 5 was subcloned into Bluescript KS(−) (Stratagene; construct 1). A 0.8-kb *Eco*RI–*Xba*I fragment containing exon 2, which is 67 nucleotides in size and contains the ATG start codon as well as the signal peptide of β1 integrin was subcloned into Bluescript KS(−) (construct 2). An *Ssp*I site was found upstream and an *Xba*I site downstream of the intron/exon boundary. The genomic DNA between these two sites was replaced by kinased and annealed oligonucleotides (90-mer oligonucleotide 1: 5′-ATTTTCTCTATCAATAATAATATA-CATTTTCTGTTATAG*ATG*GGATTCGGCCATTGAACAA-GATGGATTGCACGCAGGTTCTCCGGCCGCT-3′; 94-mer oligonucleotide 2: 5′-CTAGAGCGGCCGGAGAACCTGCGT-GCAATCCATCTTGTTCAATGGCCGAATCCCATCTATA-ACAGAAAATGATATTATTATTGATAGAGAAAAT-3′) that contain the *Ssp*I site, a 5′-DNA overhang fitting to the *Xba*I site, the remaining intronic sequence,the β1 integrin start codon and in-frame the initial 48 nucleotides of the *neo* gene (from ATG to the *Eag*I site of the *neo* gene; construct 3). After confirming the integrity of the inserted oligonucleotides by sequence analysis, the DNA was digested with *Xba*I, filled in with dNTPs by Klenow fragment, and digested afterwards with *Eag*I for inserting the *Eag*I-filled *Sal*I fragment of the neomycin gene released from pMC1*neo*pA (construct 4). With the insertion of the *neo* gene, construct 4 has gained a new *Bam*HI and *Sal*I site. Construct 4 was cleaved with both enzymes and a *Bam*HI–*Sal*I fragment from pKO*geo*21 (Fässler et al. 1995) containing exon 2 without start codon and intron 2 up to the *Sal*I site was inserted (construct 5). In the last cloning step construct 1 was digested with *Eco*RI and *Sal*I and ligated with the *Eco*RI–*Sal*I fragment of construct 5 leading to the targeting vector pKO*neo*17.

The ES cell lines used for the establishment of knockout clones were D3 (Doetschman et al. 1985) provided by Rudolf Jaenisch (Whitehead Institute, Massachusetts Institute of Technology, Boston, MA; passage number not known), and R1 (Nagy et al. 1993) provided by Andras Nagy (Mount Sinai Hospital, Toronto, Canada; passage 9). Both cell lines were routinely cultured on a feeder layer of γ-irradiated embryonic fibroblast cells in Dulbecco's modified Eagle medium supplemented with 15% heat-inactivated fetal calf serum (GIBCO), 10^{-4}M β-mercaptoethanol (Sigma) and nonessential amino acids (GIBCO). The embryonic feeder cells were prepared from Col9a1-deficient mice (Fässler et al. 1994) and γ-irradiated (1500 rad for 30 min) before plating.

About 1×10^8 D3 ES cells were electroporated with 150 μg of *Cla*I-linearized targeting vector pKO*neo*17 and ~6×10^7 D3 or R1 ES cells were electroporated with 90μg of *Not*I linearized targeting vector pKO*geo*21, respectively, using a Bio-Rad Gene Pulser set at 800 V and 3 μF. After 24 hr without selection, G418 (300 μg/ml of dry powder; GIBCO) was added to the culture medium. After another 8–11 days, colonies were picked into 24-well dishes (Costar) and expanded. Half of the 24-well dish was frozen, and the other half was used to isolate DNA for Southern blot analysis (Laird et al. 1991). The colonies were screened individually by cleaving genomic DNA with *Bam*HI and probing the Southern blots with the external probe A (*Bam*HI–*Eco*RV fragment), a 800-bp fragment that contains intron sequence (Fig. 1).

Generation of β1 integrin-deficient and chimeric mice

Blastocysts were isolated at day 3.5 p.c. from C57BL/6 mice, injected with 15 ES cells as described by Bradley (1987), and transferred into the uterus of pseudopregnant recipient (C57BL/6×DBA)F_1 females (2.5 days p.c.). Chimeric mice were mated with C57BL/6 females to test for germ-line transmission or with 129sv females to obtain inbred lines carrying the mutated β1 integrin alleles.

Southern and Northern blot analysis

Southern blots were prepared from ES cell or tail DNA (Laird et al. 1991), digested with restriction enzymes (Boehringer Mannheim), and electrophoresed through a 0.7% agarose gel. Hybridization was carried out with a ^{32}P-labeled genomic 0.8-kb *Bam*HI–*Eco*RI fragment (Fig. 1A) prepared by random primer labeling (followed the protocol of Primelt, Stratagene).

For Northern blots, total RNA was isolated from liver, kidney, and brain of 8-week-old normal and β1 $^{+/-}$ mice as described by Auffray and Rougeon (1980). RNA was separated electrophoretically, blotted onto Zetabind membrane (Bio-Rad Laboratories), UV cross-linked and probed in Church buffer (Church and Gilbert 1984) at 65°C. Filters were washed twice in 0.2× SCC, 1% SDS, at 65°C and exposed to X-ray film for 24 or 72 hr at −80°C.

The following oligolabeled probes were used: mouse β1 integrin cDNA (obtained from R. O. Hynes, Massachusetts Institute of Technology, Boston, MA) and mouse cDNA for β-actin (Fässler et al 1995).

Microscopic anatomy

Freshly dissected embryo implantation chambers (6.5, 7.5, 8.5, and 10.5 days postcoitum) or tissues were surgically removed, frozen on dry ice, and stored at −80°C. Tissue sections were prepared from four 6- to 10-week-old male chimeric mice that were transcardially perfused with PBS followed by 4% paraformaldehyde, 0.02% NaN_3. After a short postfixation and equilibrium in 30% sucrose, the tissue was embedded in OCT compound (Miles), frozen in dry-ice–pentane, and stored at −80°C.

Embryos and tissues were cut at 10–20 μm on a Leitz cryostat and collected on gelatine-coated slides. *lacZ* staining followed published protocols (Fässler et al. 1995). To avoid detection of endogenous β-galactosidase activity, solutions were adjusted to pH 7.6 and incubation was done at 30°C overnight. Control of these parameters prevents detection of the endogenous enzyme in the mouse nervous system (K. Müllhofer and M. Meyer, unpubl.).

Counterstaining with neutral red, cresyl violet, or eosin was performed according to standard histological techniques with minor modifications. Xylol was replaced with Histoclear (National Diagnostics, Atlanta), and the sections were covered with Canada balsam and coverslipped.

Immunohistochemistry

β1 $^{+/-}$ mice were intercrossed and blastocysts were collected on E3.5 p.c. After the removal of the zona pellucida by acid Tyrode's solution (pH 2.1), blastocysts were washed several times in PBS and fixed in 4% paraformaldehyde.

Immunofluorescence staining of blastocysts was done in solution using depression slides. First, antibody was a rabbit polyclonal IgG fraction (Bottger et al. 1989) specifically reacting with mouse β1 integrin. Incubation was 2 hr at room temperature. Secondary antibodies were Cy3 goat anti-rabbit IgG or FITC goat anti-rabbit IgG (Jackson ImmunoResearch Laboratories Inc., West Grove, PA). Incubation was for 1 hr at room temperature. After washing three times with PBS, blastocysts were examined with a Zeiss Axiophot microscope and subsequently stained for *lacZ* activity and photographed again. Tissue specimens were also stained with antibodies reacting specifically with mouse β1 integrin, embedded in gelvatol (Fässsler et al. 1995), and examined with a Zeiss Axiophot microscope.

Immunofluorescence staining of brain sections was done according to standard procedures using monoclonal antibodies against calbindin D28k (Swant, Fribourg, Switzerland), MAP5, and neurofilament heavy chain (both purchased from Boehringer Mannheim, Germany).

GPI assay

Separation and detection of GPI isoenzymes were performed essentially as described (Bradley 1987). Titan III Zip Zone cellulose acetate plates (Helena Laboratories) were soaked in Tris-glycine buffer (25 mM Tris-HCl at pH 8.5, 200 mM glycine) for 30 min prior to application of samples. Samples were prepared by homogenizing tissues in ~10 volumes of water with a micropestle. Cells were then lysed by at least three rounds of freezing and thawing. Samples were electrophoresed for 1.5 hr at 200 V and 4°C. Ten milliliters of 1.2% agarose containing 20 mg of fructose-6-phosphate (F6P), 2 mg β-nicotinamide adenine dinucleotide phospahte (NADP), 0.25 mg of phenazine methosulfate (PMS), and 2 mg of methylthiazolium tetrazolium (MTT) at 55°C were mixed with 1.4 units of glucose-6-phosphate dehydrogenase (G6P-DH) and poured over the gel. The GPI isoenzyme bands appeared after a few minutes. Relative levels of the two GPI isoforms were quantified densitometrically.

Whole embryos were tested after isolation of embryos from implantation chambers 8.5 days p.c. The following tissues were analyzed from 3-month-old chimeric mice: brain hemispheres, cerebellum, lung, kidney, adrenal gland, liver, spleen, testis, M. triceps, M. quadriceps, heart, and gut.

Acknowledgments

We thank Dr. Rupert Timpl for his support and valuable comments on the manuscript, Staffan Johansson for the antibody gift, Stefan Benkert for expert technical assistance and Karin Müllhofer and Andrea Steinberg for help and advice with histology. We also appreciate and acknowledge L. Stephens et al. (this issue) for sharing data prior to publication and critically reading our manuscript. This work was supported by the Deutsche Forschungsgemeinschaft (Fa-296/1-1).

The publication costs of this article were defrayed in part by payment of page charges. This article must therefore be hereby marked "advertisement" in accordance with 18 USC section 1734 solely to indicate this fact.

References

Almeida, E., M. Huovila, A. Sutherland, A. Sonnenberg, R. Calarco, D. Myles, P. Primakoff, and J.M. White. 1995. Mouse egg integrin $\alpha_6\beta_1$ funtions as a sperm receptor. *Cell* (in press).

Armant, D.R., H.A. Kaplan, and W.J. Lennarz. 1986. Fibronectin and laminin promote in vitro attachment and outgrowth of mouse blastocyst. *Dev. Biol.* **116:** 519–523.

Auffray, C. and F. Rougeon. 1980. Purification of mouse immunoglobulin heavy-chain messenger RNAs from total myeloma tumor RNA. *Eur. J. Biochem.* **107:** 303–314.

Blobel, C.P., T.G. Wolfsberg, C.W. Turck, D.G. Myles, P. Primakoff, and J.M. White. 1992. A potential fusion peptide and an integrin ligand domain in a protein active in sperm-egg fusion. *Nature* **356:** 248–252.

Bonner-Fraser, M. 1986. An antibody to a receptor for fibronectin and laminin perturbs cranial neural crest development in vivo. *Dev. Biol.* **117:** 528–536.

Bottger, B.A., U. Hedin, S. Johansson, and J. Thyberg. 1989. Integrin-type fibronectin receptors of rat arterial smooth muscle: Isolation, partial characterization and role in cytoskeletal organization and control of differentiated properties. *Differentiation* **41:** 158–167.

Bradley, A. 1987. Production and analysis of chimeric mice. In *Teratocarcinomas and embryonic stem cells: A practical approach* (ed. E. J. Robertson), pp. 113–151. IRL Press, Oxford, UK.

Brown, D.G., V.N. Warren, P. Pahlsson, and S.J. Kimber. 1993. Carbohydrate antigen expression in murine embryonic stem cells and embryos: I. Lacto and neo-lacto determinants. *Histochem. J.* **25:** 452–461.

Brown, J.J.G., and V.E. Papaioannou. 1993. Ontogeny of hyaluronan secretion during early mouse devlopment. *Development* **117:** 483–492.

Carson, D.D., J.-P. Tang, and J. Julian. 1993. Heparan sulfate proteoglycan (perlecan) expression by mouse embryos during acquisition of attachment competence. *Dev. Biol.* **155:** 97–105.

Chen, J., Y. Shinkai, F. Young, and F.W. Alt. 1994. Probing immune functions in RAG-deficient mice. *Curr. Opin. Immunol.* **6:** 313–319.

Church, G.M. and W. Gilbert. 1984. Genomic sequencing. *Proc. Natl. Acad. Sci.* **81:** 1991–1994.

Damsky, C., A. Sutherland, and S. Fisher. 1993. Extracellular matrix 5: Adhesive interactions in early mammalian embryogenesis, implantation, and placentation. *FASEB J.* **7:** 1320–1329.

Dariberre, T., K.M. Yamada, K.E. Johnson, and J.C. Boucaut. 1984. The 140-kDa fibronectin receptor complex is required for mesodermal cell adhesion during gastrulation in the amphibian *Pleurodeles waltii*. *Dev. Biol.* **126:** 182–194.

DeSimone, D.W. 1994. Adhesion and matrix in vertebrate development. *Curr. Opinion Cell Biol.* **6:** 747–751.

Doetschman, T. C., H. Eistetter, M. Katz, W. Schmidt, and R. Kemler. 1985. The in vitro development of blastocyst-derived embryonic stem cell lines: Formation of visceral yolk sac, blood islands and myocardium. *J. Embryol. Exp. Morphol.* **87:** 27–45.

Drake, C.J., L.A. Davis, J.E. Hungerford, and C.D. Little. 1992a. Perturbation of b1 integrin-mediated adhesions results in altered somite cell shape and behavior. *Dev. Biol.* **149:** 327–338.

Drake, C.J., L.A. Davis, and C.D. Little. 1992b. Antibodies to β1 integrin cause alteration of aortic vascologenesis in vivo. *Dev. Dynam.* **193:** 83–91.

Ernsberger, U., D. Edgar, and H. Rohrer. 1989. The survival of early chick sympathetic neurons in vitro is dependent on a suitable substrate but independent of NGF. *Dev. Biol.* **135:** 250–262.

Fässler, R., P.N.J. Schnegelsberg, J. Dausman, T. Shinya, Y. Muragaki, M.T. McCarthy, B.R. Olsen, and R. Jaenisch. 1994. Mice lacking a1(IX) collagen develop non-inflammatory degenerative joint disease. *Proc. Natl. Acad. Sci.* **91:** 5070–5074.

Fässler, R., M. Pfaff, J. Murphy, A.N. Noegel, S. Johannson, R. Timpl, and A. Albrecht. 1995. The lack of β1 integrin gene in embryonic stem cells affects cell morphology, migration and adhesion but not integration into the inner cell mass of blastocysts *J. Cell Biol.* **128:** 979–988.

Galileo, D.S., J. Majors, A.F. Horwitz, and J.R. Sanes. 1992. Retrovirally transduced antisense integrin RNA inhibits neuroblast migration in vivo. *Neuron* **9:** 117–131.

Gu, H., J.D., Marth, P.C. Orban, H. Mossmann, and K. Rajewsky. 1994. Deletion of a DNA polymerase β gene segment in T cells using cell type-specific gene targeting. *Science* **265:** 103–106.

Gurtner, G.C., V. Davis, H. Li, M.J. McCoy, A. Sharpe, and M.I. Cybulsky. 1995. Targeted disruption of the murine VCAM1 gene: Essential role of VCAM-1 in chorioallantoic fusion and placentation. *Genes & Dev.* **9:** 1–14.

Hynes, R.O. 1992. Integrins: Versatility, modulation, and signalling in cell adhesion. *Cell* **69:** 11–25.

Jacobs, A.L., and D.D. Carson. 1991. Proteoglycan synthesis and metabolism by mouse uterine stroma cultured in vitro. *J. Biol. Chem.* **266**:15464–15469.

Jaffredo, T., A.F. Horwitz, C.A. Buck, P.M. Rong, and F. Dieterlen-Lievre. 1988. Myoblast migration specifically inhibited in the chick embryo by grafted CSAT hybridoma cells secreting an anti-integrin antibody. *Development* **103:** 431–446.

Kalcheim, C., Y.-A. Barde, H. Thoenen, and N.M. LeDouarin. 1987. In vivo effect of brain-derived neurotrophic factor on the survival of developing dorsal root ganglion cells. *EMBO J.* **6:** 2871–2873.

Kwee, L., H.S. Baldwin, H.M. Shen, C. Stewart, C. Buck, C.A. Buck, and M.A. Labow. 1995. Defective development of the embryonic and extraembryonic circulatory systems in vascular cell adhesion molecule (VCAM-1) deficient mice. *Development* **121:** 489–503.

Laird, P.W., A. Zijderveld, K. Linders, M.A. Rudnicki, R. Jaenisch, and A. Berns. 1991. Simplified mammalian DNA isolation procedure. *Nucleic Acids Res.* **19:** 4293.

Letourneau, P.C., I.V. Pech, S.L. Rogers, S.L. Palm, J.B. McCarthy, and L.T. Furcht. 1988. Growth cone migration across extracellular matrix components depends on integrin, but migration across glioma cells does not. *J. Neurosci. Res.* **21:** 286–297.

Menko, A.S. and D. Boettiger. 1987. Occupation of the extracellular matrix receptor, intergin, is a control point for myogenic differentiation. *Cell* **51:** 51–57.

Nagy, A., J. Rossant, R. Nagy, W. Abramow-Newerly, and J.C. Roder. 1993. Derivation of completely cell culture-derived mice from early-passage embryonic stem cells. *Proc. Natl. Acad. Sci.* **90:** 8424–8428.

Richa, J., C.H. Damsky, C.A. Buck, B.B. Knowles, and D. Solter. 1985. Cell surface glycoproteins mediate compaction, trophoblast attachment, and endoderm formation during early mouse development. *Dev. Biol.* **108:** 513–521.

Rosen, G.D., J.R. Sanes, R. LaChance, J.M. Cunningham, J. Roman, and D.C. Dean. 1992. Roles for the integrin VLA-4 and its counter receptor VCAM-1 in myogenesis. *Cell* **69:** 1107–1119.

Ruoslahti, E., and J.C. Reed. 1994. Anchorage dependence, integrins, and apoptosis. *Cell* **77:** 477–478.

Sastry, S.K., and A.F. Horwitz. 1993. Integrin cytoplasmic domains: mediators of cytoskeletal linkages and extra- and intracellular initiated transmembrane signalling. *Curr. Opin. Cell Biol.* **5:** 819–831.

Stephens, L.E., A.E. Sutherland, I.V. Klimanskaya, A. Andrieux, J. Meneses, O. Behrendtsen, R.A. Pedersen, and C.H. Damsky. 1995. Deletion of β1 integrins in mice results in inner cell mass failure and periimplantation lethality. *Genes & Dev.* (this issue).

Sutherland, A.E., P.G. Calarco, and C.H. Damsky. 1988. Expression and function of cell surface extracellular matrix receptors in mouse blastocyst attachment and outgrowth. *J. Cell Biol.* **106:** 1331–1348.

———. 1993. Developmental regulation of integrin expression at the time of implantation in the mouse embryo. *Development* **119:** 1175–1186.

Thiery, J.P., J.L. Duband, and G.C. Tucker. 1985. Cell migration in the vertebrate embryo: Role of cell adhesion and tissue environment in pattern formation. *Annu. Rev. Cell Biol.* **1:** 91–113.

Tomaselli, K.J., K.M. Neugebauer, J.L. Bixby, J. Lilien, L.F. Reichardt. 1988. N-cadherin and integrins: Two receptor systems that mediate neuronal process outgrowth on astrocyte surfaces. *Neuron* **1:** 33–43.

Yang, J.T., H. Rayburn, and R.O. Hynes. 1993. Embryonic mesodermal defects in α5 integrin-deficient mice. *Development* **119:** 1093–1105.

———. 1995. Cell adhesion events mediated by α4 integrins are essential in placental and cardiac development. *Development* **121:** 549–580.

Consequences of lack of beta 1 integrin gene expression in mice.

R Fässler and M Meyer

Genes Dev. 1995, **9:**
Access the most recent version at doi:10.1101/gad.9.15.1896